https://ntrs.nasa.gov/search.jsp?R=19930085186 2020-06-17T15:40:20+00:00Z

NACA TN 4400

NATIONAL ADVISORY COMMITTEE FOR AERONAUTICS

TECHNICAL NOTE 4400

MEASUREMENTS OF GROUND-REACTION FORCES AND VERTICAL CENTER-OF-GRAVITY ACCELERATIONS OF A BOMBER AIRPLANE TAXIING OVER OBSTACLES

By James M. McKay, Richard H. Sawyer, and Albert W. Hall

Langley Aeronautical Laboratory
Langley Field, Va.

Washington

September 1958

NATIONAL ADVISORY COMMITTEE FOR AERONAUTICS

TECHNICAL NOTE 4400

MEASUREMENTS OF GROUND-REACTION FORCES AND VERTICAL CENTER-OF-GRAVITY ACCELERATIONS OF A BOMBER AIRPLANE TAXIING OVER OBSTACLES

By James M. McKay, Richard H. Sawyer, and Albert W. Hall

SUMMARY

An investigation was made on an unswept-wing four-engine bomber airplane to determine the vertical and drag ground-reaction forces imposed on the landing gear when taxiing over obstacles 1.5 and 3.0 inches in height and 1, 2, and 4 feet in width. Vertical accelerations at the center of gravity of the airplane and shock-strut displacement were also measured. The investigation included a range of ground speeds from 10 to 70 miles per hour. The weight of the airplane was approximately 95,000 pounds. Results are presented of the effects of ground speed and the widths and heights of the obstacles on the vertical and drag forces, on vertical acceleration at the center of gravity of the airplane, on shock-strut displacement, and on response of the upper mass of the airplane structure.

The results of the investigation indicate that maximum incremental vertical and rearward drag ground-reaction forces are primarily a function of the height of the obstacle. The maximum incremental vertical ground-reaction force for each obstacle height tested was the greatest for the 2- and 4-foot widths and the smallest for the 1-foot width. The maximum rearward drag ground-reaction force for each obstacle height tested was the greatest for the 1-foot-wide obstacles and the smallest for the 4-foot-wide obstacles. The maximum incremental shock-strut compression was greatest for the 3.0-inch-high obstacles and increased with obstacle width for both the 1.5- and 3.0-inch-high obstacles. The ground-reaction forces imposed on the main-landing-gear wheels are not affected because the nose wheel strikes the obstacles first. The center-of-gravity vertical acceleration of the airplane was the highest for the 2- and 4-foot-wide obstacles for both the 1.5- and 3.0-inch heights tested. The dynamic response factor at the center of gravity of the airplane, as a result of taxiing over any of the obstacles tested at speeds above 25 miles per hour, reached values as much as twice the mean value of 1.0 obtained in some previous landing tests at vertical velocities up to about 5.5 feet per second. These higher values of dynamic response factor obtained in the obstacle tests appeared to be associated with higher force-input rates which, at the higher speeds, reached values over three times the force-input rate obtained in the previous landing tests.

INTRODUCTION

In recent years considerable need has existed for experimental data which airplane designers could use to define more accurately the ground-reaction forces imposed on airplanes taxiing under abnormal or severe conditions. Only a limited amount of experimental data defining these ground-reaction forces under actual taxiing conditions have been available. Inasmuch as there was available a bomber airplane being used for a landing-loads investigation (ref. 1), it was considered that additional useful data could be obtained by taxiing the airplane at various speeds over obstacles of various widths and heights. Although the airplane was instrumented primarily to measure the vertical and drag ground-reaction forces on the main gear during landing instead of the response of the wing and fuselage components to dynamic loads, it was considered that the ground-reaction force data would still be of value in indicating the input loads developed on this type of airplane when taxiing over obstacles.

This investigation included the measurement of the ground-reaction forces on the main landing gear, the vertical acceleration at the center of gravity of the airplane, and the shock-strut displacement when taxiing at various speeds over obstacles of various widths and heights.

SYMBOLS

Δa	maximum incremental vertical center-of-gravity acceleration, ft/sec^2
ΔF_h	maximum rearward drag ground-reaction force, lb
ΔF_v	maximum incremental vertical ground-reaction force, lb
$\Delta F_{v,t}$	maximum total incremental vertical ground-reaction force, lb
g	acceleration due to gravity, ft/sec^2
h	height of obstacle, in.
$t_{\Delta a}$	time from impact for center-of-gravity vertical acceleration to reach peak value, sec
t_{F_h}	time from impact for rearward drag ground reaction to reach peak value, sec

t_{F_v}	time from impact for vertical ground reaction to reach peak value, sec
$t_{\delta_{max}}$	time from impact for shock-strut displacement to reach peak value, sec
$\Delta t_{\delta_{max}}$	increment in time from start of shock-strut displacement to peak value, sec
V	ground speed, mph
W	weight of airplane, lb
W_w	static vertical load on wheel, lb
w	width of obstacle, ft
$\Delta\delta_{max}$	maximum incremental shock-strut displacement, in.

EQUIPMENT, TESTS, AND INSTRUMENTATION

An unswept-wing four-engine bomber airplane (fig. 1) together with a series of obstacles 1, 2, and 4 feet wide and 1.5 and 3.0 inches high (figs. 2 and 3) were used in the tests. The obstacles were built up of $\frac{3}{4}$-inch plywood and were bolted to the runway with their center lines 300 feet apart along the runway. The positions of the obstacles allowed the nose gear to strike the center obstacle first and the main wheels to strike the outer obstacles later. The weight of the airplane for these tests was approximately 95,000 pounds, and the corresponding tire pressure for this weight was 75 pounds per square inch for the 56-inch-diameter smooth-contour main-wheel tires. The main-gear shock struts had a total stroke of 12 inches and were adjusted by air pressure to a position 2 inches from fully compressed with the airplane fully loaded.

The airplane was taxied over the obstacles at ground speeds ranging from 10 to 70 miles per hour in both directions along the runway. Several tests were made with the 3-inch-high-nose wheel obstacles removed in order to determine whether the impact with the obstacle by the nose gear had any effect on the main-gear impact with the obstacle.

Figure 4 shows a sketch of one of the main-landing-gear trucks (a pair of wheels referred to as a unit) with one wheel removed. The strain gages and the vertical and horizontal linear accelerometers used in obtaining vertical and drag ground-reaction forces for each of the four

main wheels were located as shown. The linear accelerometers had natural frequencies in the range from 160 to 220 cycles per second. The strain-gage and linear-accelerometer outputs were recorded on two photographically recording oscillographs using galvanometers having a natural frequency of 150 cycles per second. Vertical acceleration was measured at the center of gravity of the airplane by means of a photographically recording accelerometer having a natural frequency of 12 cycles per second. Shock-strut deflections were measured by means of slide-wire position transmitters and photographically recording oscillographs using galvanometers having a natural frequency of 9 cycles per second.

DATA REDUCTION

For each wheel the axle strain-gage measurements were used to calculate vertical and drag forces on the axle. A complete description of the method of obtaining the forces on the axle from the strain-gage measurements is given in reference 1. The vertical and drag ground-reaction forces for each wheel were then determined by adding to the corresponding axle force an inertia term consisting of the product of the mass outboard of the strain-gage location and the appropriate acceleration as measured by the linear accelerometers.

The actual ground speed over the obstacles was calculated by using the relation of the interval between the time the nose wheel and the main wheel struck the obstacle and the distance between the nose wheel and the main wheels. This time interval was determined from the oscillograph records by noting the times of impact with the obstacle as indicated by the vertical accelerometers mounted on the nose and main gears. The ground speeds for the tests with the nose-wheel obstacles removed were calculated from rotational velocities of the main wheels which were obtained from motion-picture records of the main wheels. For some of the tests with the nose-wheel obstacles in place, both methods of calculating ground speed were used, and the results compared favorably.

RESULTS AND DISCUSSION

Typical time histories of vertical and drag ground-reaction forces, vertical acceleration at the center of gravity of the airplane, and shock-strut displacement are shown in figure 5 for the left outboard wheel as it rolled over obstacles 3 inches high and 1, 2, and 4 feet in width at a ground speed of approximately 70 miles per hour.

For the time histories shown in figure 5, both the vertical and drag forces reached maximum values at approximately the same time; namely, between 0.025 and 0.03 second after impact with the obstacles for all three widths of the obstacles tested. The time for the vertical acceleration at the center of gravity to reach a peak value can be seen to be somewhat longer; that is, about 0.035 to 0.045 second. For the shock strut, the time to reach a peak deflection varied from about 0.06 to 0.08 second. These times appear to be typical of the times required for the forces, acceleration, and shock-strut displacement to reach peak values at moderate and high speeds. The maximum incremental values of the force and the times for each of these values to reach a peak after impact are given in table I for each individual wheel. Table II gives the maximum total incremental values of the vertical forces on all four wheels, the incremental center-of-gravity vertical accelerations, and the times for these quantities to reach peak values. The maximum total vertical forces given in table II were determined by summing the individual vertical-force time histories and are, therefore, not equivalent to the sum of the maximum individual vertical forces given in table I. Table III gives some of the shock-strut time-history characteristics.

Ground-Reaction Forces

The variation with ground speed of the maximum incremental vertical and maximum rearward drag forces caused by impact with the obstacle are shown in figure 6 for all of the obstacles tested for the left outboard wheel only. The data for the other three main wheels indicated the same trends as the data for the left outboard wheel and are presented in table I.

For each particular width tested the highest vertical forces (fig. 6(a)) occurred for the 3.0-inch-high obstacle. For both the 1.5- and 3.0-inch-high obstacles the 2- and 4-foot widths resulted in higher vertical forces than the 1-foot width. In this connection it was observed from motion pictures taken of the wheel that for the 1-foot-wide obstacles the tires completely engulfed the obstacle and the wheel did not appreciably rise as it passed over the obstacle. For the drag force (fig. 6(b)) the opposite results were indicated in that the higher drag forces occurred for the 1-foot-wide obstacles for each particular height tested, with the values decreasing as the obstacle width increased. The highest values of drag force occurred for the 3-inch-high obstacles.

The vertical and drag forces increased with an increase in ground speed up to 40 to 60 miles per hour (depending on obstacle height), after which these values had a tendency to decrease with ground speed. For the tests with the 4-foot-wide obstacles the motion pictures indicated that the wheel rose up on the obstacle and that the complete footprint was supported by the obstacle part of the time during the passage of the wheel over the obstacle. Thus, the ground-reaction forces for the 4-foot-wide obstacles probably closely represent those which would be experienced

when taxiing back onto a runway having a shoulder height equivalent to that of the obstacles tested. The faired curve representing results for the 1-foot-wide obstacles for both heights are also shown in figure 7 as the variation of vertical and drag load factor with speed, where load factor is simply the maximum incremental ground-reaction force divided by the static vertical load on the wheel. Results in terms of load factor (furnished by the manufacturer) obtained from strain-gage measurements on the main vertical landing-gear strut of an unswept-wing ten-engine heavy bomber airplane for tests at two weights over obstacles of the same width and heights are also shown. The results shown for the heavy bomber are not directly comparable to the results of the present tests and are presented only to indicate trends. The strut forces measured in the tests of the heavy bomber would have to be converted to ground-reaction forces by correction for the unknown inertia forces of the mass below the point of measurement in order to be comparable. As far as trends are concerned, however, the measurements shown for the heavy bomber do not seem to indicate the same variations with speed as do the present results but do agree in indicating higher values of both drag and vertical load factor for the higher obstacle.

Center-of-Gravity Acceleration

From the time histories of the center-of-gravity vertical acceleration such as shown in figure 5, the maximum incremental values were obtained for each impact with an obstacle and are given in table II. The variation of the maximum incremental vertical acceleration with ground speed is shown in figure 8 for the various obstacles tested. These data varied with ground speed in a somewhat similar manner as the vertical forces (fig. 6) with the highest values of acceleration occurring for the 1.5- and 3.0-inch-high obstacles of 2- and 4-foot widths.

A comparison of these vertical-acceleration results with those available from the obstacle tests of the heavy bomber is shown in figure 9. The tests of the heavy bomber included 1.5- and 3.0-inch-high obstacles 1-foot wide for two airplane weights. The vertical accelerations for the heavy bomber were measured at the fuselage center line on the rear spar of the wing in close proximity to the center of gravity of the airplane. For both the heavy bomber and the airplane used in the present tests, the ground-reaction forces were transferred to the structure through wing-mounted landing gear. The results for the heavy bomber show about the same values up to speeds of 20 to 30 miles per hour, but at higher speeds the results show lower values than do the results of the present tests.

The incremental vertical-acceleration results of the present tests are compared in figure 10 with those obtained from the manufacturer for obstacle tests of a swept-wing medium bomber which had six jet engines and weighed 95,000 pounds. Results are shown for both the forward and

rearward gears of the bicycle-gear arrangement as the bomber passed over each obstacle. The results for the medium bomber are for slightly higher (1.6-inch) and wider (2.2- and 4.5-foot) obstacles than are the present results. The results for the forward gear of the medium bomber show the same increase with speed at the lower speeds as do the results of the present tests but, in general, go to higher values at speeds in the range of 40 to 60 miles per hour. The results for the rearward gear are of the same order at 15 miles per hour as the present results but are considerably lower at higher speeds.

As has been previously shown (fig. 9) the vertical center-of-gravity response was generally lower for the larger, more flexible heavy bomber than for the airplane used in the present tests. In contrast, the swept-wing medium bomber which had the landing gear mounted in the fuselage indicated a center-of-gravity response for the forward-gear impacts higher than that for the airplane used in the present tests. These contrasting results only serve to emphasize that the response at the center of gravity is dependent on a number of factors such as the landing-gear shock-strut characteristics, the location of the landing gear, the mode shape excited, and the flexibility of the structure.

Shock-Strut Displacement

From the time histories of shock-strut displacement such as are shown in figure 5, the maximum incremental values of compression were obtained for both the left and right main gear for each impact with an obstacle. The variation of the peak incremental compression with speed is shown in figure 11 for the various obstacles used in the tests. For the 1.5-inch-high obstacles it appears that the compression increases with both speed and obstacle width. The large amount of scatter of the results at the lowest speed appeared to be associated with the rolling of the airplane caused by one gear rising on an obstacle before the other. For the 3.0-inch-high obstacles it is evident that the shock-strut displacement is higher than that for the 1.5-inch-high obstacles and increases with obstacle width as for the 1.5-inch-high obstacles but varies rather erratically with speed.

Examination of the time histories of shock-strut motion indicated that in most cases the time history appeared to be similar in shape to a sine curve for the initial motion up to the peak value of compression. Because of sticking tendencies, motion of the shock strut, in general, did not start at the time of impact; therefore, both the values of the time from impact to peak displacement and the time from start of shock-strut motion to peak displacement are given in table III together with the value of the maximum incremental shock-strut displacement.

Effects of Nose Wheel and Runway Roughness

From strain-gage and accelerometer records it was observed that with the 300-foot spacing between the obstacles the impact with one obstacle did not appear to have any significant effect on the impact with the next obstacle. A comparison of results with and without the nose-wheel obstacles in place (figs. 6 and 8) indicates that the nose-wheel impact with the obstacles has no significant effect on the main-gear ground-reaction forces and the vertical acceleration at the center of gravity of the airplane. In addition, runway roughness encountered throughout the investigation transmitted loads through the landing gear to the airplane structure and resulted in wing and engine oscillations which, depending on the phasing at the time of obstacle impact, either added to or subtracted from the loads contributed by the obstacle. These wing and engine oscillations are believed to have contributed to the scatter of the ground-reaction force and center-of-gravity vertical-acceleration data.

Center-of-Gravity Dynamic Response Factor

The response of the upper mass of the airplane structure caused by the landing-gear trucks striking the obstacles was analyzed and compared with the response of the upper mass obtained from landing impacts during a landing-loads investigation made previously with this airplane (ref. 1). This analysis was made on the basis of a dynamic response factor which was taken as $\frac{W\,\Delta a}{g\,\Delta F_{v,t}}$

where

W weight of airplane

$\Delta F_{v,t}$ maximum total incremental vertical force applied to main gear by impact with obstacle or in landing impact

Δa maximum incremental vertical center-of-gravity acceleration

The variation of the response factor with ground speed for the results obtained in the obstacle tests is shown in figure 12(a). For the landing tests the response factor is given as a function of the vertical velocity at impact in figure 12(b). A comparison of these results indicates that for vertical velocities up to 5.5 feet per second in the landing tests, the response factor is low (mean value about 1.0) and agrees with the response factor obtained in the obstacle tests at the low speeds below about 25 miles per hour. For the obstacle tests made at higher speeds, the response factor is, in general, greater and

reaches values as much as twice the mean value obtained in the landing tests.

The higher value of the response factor shown by the results of the obstacle tests (at the higher speeds), when compared with the results of the landing tests, is apparently associated with the higher force-input rate that occurred during the high-speed obstacle test. The variation of force-input rate with ground speed for the obstacle tests is given in figure 13(a). The force-input rate variation with vertical velocity for the landing impacts is shown in figure 13(b). These results indicate that the force-input rate increases with increasing ground speed or with increasing vertical velocity. The maximum force-input rates obtained in the obstacle tests (for example 2,950,000 lb/sec at 65 miles per hour) were over three times as high as those obtained in the landing impacts (830,000 lb/sec at about 5.5 feet per second). It is also evident that for the landing impacts the force-input rates are comparable to those for the obstacle tests up to 30 miles per hour.

The relationship between dynamic response factor and force-input rate for both the obstacle and landing tests is shown in figure 14. It appears that, in general, the dynamic response factor increases with an increase in force-input rate. The values of dynamic-response factor for both the obstacle and the landing tests appear to agree throughout the range of force-input rates covered by the landing tests (0 to 830,000 lb/sec).

CONCLUSIONS

The principal results of an investigation of an unswept-wing four-engine bomber airplane taxiing at various speeds over obstacles of various widths and heights are summarized as follows:

1. Maximum incremental vertical and rearward drag ground-reaction forces which develop on impact with an obstacle are primarily a function of the height of the obstacle.

2. The maximum incremental vertical ground-reaction force for both obstacle heights tested (1.5 and 3.0 inches) was greatest for the 2- and 4-foot widths and smallest for the 1-foot width.

3. The maximum rearward drag ground-reaction force for both obstacle heights tested was greatest for the 1-foot-wide obstacle and smallest for the 4-foot-wide obstacles.

4. The maximum incremental shock-strut compression was greater for the 3.0-inch-high obstacles than for those 1.5 inches high and increased with obstacle width for both obstacle heights tested.

5. Ground-reaction forces imposed on the main-landing-gear wheels are not affected because the nose wheel strikes the obstacles first.

6. The airplane center-of-gravity vertical accelerations developed on impact with the obstacle were the highest for the 2- and 4-foot-wide obstacles for both the 1.5- and 3.0-inch heights tested.

7. The dynamic response factor at the center of gravity of the airplane as a result of taxiing over the obstacles at the higher speeds reached values as much as twice the mean value of 1.0 obtained in some previous landing tests at vertical velocities up to 5.5 feet per second. These higher values of dynamic response factor obtained in the obstacle tests appeared to be associated with higher force-input rates which, at the higher speeds, reached values over three times the highest force-input rate obtained in the landing tests.

Langley Aeronautical Laboratory,
National Advisory Committee for Aeronautics,
Langley Field, Va., July 29, 1958.

REFERENCE

1. Hall, Albert W., Sawyer, Richard H., and McKay, James M.: Study of Ground-Reaction Forces Measured During Landing Impacts of a Large Airplane. NACA TN 4247, 1958. (Supersedes NACA RM L55E12c.)

TABLE I.- GROUND-REACTION FORCES

(a) Left outboard wheel

[Nose-wheel obstacles removed for tests 49 to 60]

Test number	Ground speed, V, mph	Obstacle dimensions		Force time-history characteristics			
		w, ft	h, in.	ΔF_v	t_{F_v}	ΔF_h	t_{F_h}
1	11.9	1	1.5	7.3×10^3	0.075	4.7×10^3	0.025
2	10.0	2	↓	10.7	.120	4.7	.030
3	10.2	4		10.5	.113	4.1	.028
4	11.6	1		6.6	.045	5.0	.030
5	10.5	2		12.0	.120	5.4	.031
6	11.1	4		9.1	.111	4.1	.040
7	25.4	1	1.5	7.6	0.015	7.0	0.030
8	26.7	2	↓	12.2	.045	5.2	.025
9	27.2	4		11.1	.055	5.0	.030
10	33.4	1		8.8	.020	7.4	.030
11	31.6	2		14.1	.045	5.5	.030
12	30.2	4		10.7	.045	5.0	.028
13	44.3	1	1.5	----------	-----	----------	-----
14	45.5	2	↓	12.6	0.030	4.4	0.020
15	47.3	4		11.8	.037	4.3	.022
16	55.6	1		9.6	.024	6.8	.022
17	53.9	2		15.0	.025	5.6	.020
18	50.8	4		12.0	.032	5.3	.020
19	52.3	1	1.5	8.1	0.022	6.4	0.033
20	42.2	2	↓	12.6	.027	5.1	.022
21	43.7	4		11.7	.036	4.7	.021
22	65.0	1		10.5	.020	4.9	.020
23	62.5	2		14.3	.022	4.3	.017
24	62.5	4		12.0	.030	4.4	.020
25	12.1	1	3.0	8.3	0.045	8.8	0.027
26	8.2	2	↓	12.8	.145	7.0	.045
27	9.3	4		12.0	.130	7.3	.030
28	10.1	1		7.6	.045	8.7	.036
29	10.9	2		17.2	.115	7.6	.031
30	10.5	4		18.6	.118	7.1	.035
31	27.8	1	3.0	9.2	0.028	12.0	0.034
32	26.6	2	↓	21.4	.050	9.7	.040
33	25.8	4		17.0	.055	7.3	.025
34	29.2	1		10.6	.045	11.6	.031
35	27.0	2		19.9	.045	10.9	.027
36	26.4	4		20.7	.052	8.0	.029
37	46.1	1	3.0	9.7	0.015	12.0	0.022
38	47.3	2	↓	26.3	.030	9.4	.020
39	47.3	4		22.0	.035	9.5	.011
40	47.3	1		11.4	.020	11.6	.027
41	47.3	2		23.4	.030	11.9	.029
42	46.2	4		23.3	.032	9.0	.020
43	59.4	1	3.0	9.8	0.018	14.8	0.020
44	58.4	2	↓	22.3	.021	13.0	.024
45	62.6	4		24.5	.030	10.0	.020
46	62.6	1		11.6	.021	12.4	.021
47	62.6	2		25.8	.024	11.8	.019
48	60.4	4		25.0	.035	7.7	.020
49	38.0	1	3.0	9.9	0.028	12.9	0.043
50	36.5	2	↓	21.7	.057	8.7	.029
51	39.1	4		21.6	.055	8.9	.031
52	45.2	1		10.1	.048	10.9	.033
53	44.4	2		19.9	.050	8.6	.035
54	42.2	4		21.3	.050	7.8	.035
55	71.9	1	3.0	13.1	0.022	11.8	0.030
56	70.1	2	↓	21.7	.032	13.2	.032
57	66.5	4		22.2	.042	8.2	.024
58	68.3	1		11.8	.018	10.5	.028
59	70.1	2		24.2	.027	8.7	.027
60	70.1	4		21.3	.027	8.5	.028

TABLE I.- GROUND-REACTION FORCES - Continued

(b) Left inboard wheel

[Nose-wheel obstacles removed for tests 49 to 60]

Test number	Ground speed, V, mph	Obstacle dimensions		Force time-history characteristics			
		w, ft	h, in.	ΔF_v	t_{F_v}	ΔF_h	t_{F_h}
1	11.9	1	1.5	6.0×10^3	0.043	7.6×10^3	0.023
2	10.0	2		9.1	.105	7.2	.025
3	10.2	4		9.3	.105	6.1	.024
4	11.6	1		4.1	.023	5.7	.020
5	10.5	2		8.5	.110	7.4	.033
6	11.1	4		6.4	.090	7.1	.025
7	25.4	1	1.5	6.9	0.023	8.4	0.025
8	26.7	2		9.6	.045	8.4	.030
9	27.2	4		11.0	.045	6.6	.030
10	33.4	1		8.3	.035	7.9	.025
11	31.6	2		----------	-----	7.9	.020
12	30.2	4		9.7	.035	7.9	.020
13	44.3	1	1.5	7.6	0.020	8.8	0.013
14	45.5	2		11.2	.023	8.6	.018
15	47.3	4		11.2	.024	7.1	.019
16	55.6	1		10.0	.014	6.3	.020
17	53.9	2		11.9	.020	8.7	.012
18	50.8	4		11.7	.023	7.3	.021
19	52.3	1	1.5	6.9	0.014	7.6	0.020
20	42.2	2		16.4	.030	8.7	.025
21	43.7	4		11.6	.025	7.1	.015
22	65.0	1		10.4	.015	3.4	.010
23	62.5	2		11.5	.020	6.5	.020
24	62.5	4		12.8	.015	4.8	.013
25	12.1	1	3.0	8.2	0.046	11.0	0.030
26	8.2	2		7.0	.125	11.0	.030
27	9.3	4		6.9	.120	10.4	.030
28	10.1	1		2.1	.025	9.8	.030
29	10.9	2		13.2	.100	11.7	.030
30	10.5	4		13.9	.108	10.6	.030
31	27.8	1	3.0	9.5	0.026	12.2	0.034
32	26.6	2		11.1	.042	12.9	.020
33	25.8	4		12.8	.043	12.2	.020
34	29.2	1		9.9	.018	12.8	.028
35	27.0	2		11.9	.040	13.3	.017
36	26.4	4		19.8	.043	12.6	.026
37	46.1	1	3.0	11.1	0.015	13.6	0.018
38	47.3	2		17.3	.025	14.4	.020
39	47.3	4		18.4	.028	14.1	.017
40	47.3	1		----------	-----	15.6	.022
41	47.3	2		13.5	.018	15.7	.028
42	46.2	4		19.4	.022	14.4	.018
43	59.4	1	3.0	11.8	0.005	14.0	0.020
44	58.4	2		16.7	.020	15.7	.015
45	62.6	4		22.2	.020	14.8	.015
46	62.6	1		9.3	.013	16.9	.018
47	62.6	2		14.4	.020	16.5	.020
48	60.4	4		9.1	.013	14.7	.018
49	38.0	1	3.0	10.2	0.030	13.3	0.030
50	36.5	2		14.1	.050	14.2	.020
51	39.1	4		14.2	.041	14.4	.021
52	45.2	1		12.0	.020	13.0	.018
53	44.4	2		14.0	.040	14.3	.020
54	42.2	4		16.1	.037	13.0	.020
55	71.9	1	3.0	----------	-----	----------	-----
56	70.1	2		17.5	0.028	17.3	0.028
57	66.5	4		20.4	.023	15.7	.020
58	68.3	1		12.0	.018	13.6	.018
59	70.1	2		20.9	.027	13.8	.017
60	70.1	4		15.5	.030	13.6	.020

TABLE I.- GROUND-REACTION FORCES - Continued

(c) Right outboard wheel

[Nose-wheel obstacles removed for tests 49 to 60]

Test number	Ground speed, V, mph	Obstacle dimensions		Force time-history characteristics			
		w, ft	h, in.	ΔF_v	t_{F_v}	ΔF_h	t_{F_h}
1	11.9	1	1.5	6.2×10^3	0.055	7.2×10^3	0.040
2	10.0	2		9.8	.117	4.7	.034
3	10.2	4		7.0	.110	4.9	.032
4	11.6	1		6.3	.051	6.2	.031
5	10.5	2		11.5	.105	5.4	.032
6	11.1	4		8.9	.085	5.5	.033
7	25.4	1	1.5	6.3	0.016	7.6	0.033
8	26.7	2		11.7	.050	4.8	.018
9	27.2	4		10.8	.051	5.0	.039
10	33.4	1		6.3	.030	5.6	.032
11	31.6	2		12.6	.040	5.3	.028
12	30.2	4		11.0	.050	6.1	.035
13	44.3	1	1.5	5.4	0.030	6.7	0.019
14	45.5	2		10.5	.023	4.8	.019
15	47.3	4		11.8	.031	4.1	.014
16	55.6	1		7.1	.020	3.8	.016
17	53.9	2		12.0	.017	4.0	.015
18	50.8	4		11.6	.033	5.1	.024
19	52.3	1	1.5	7.1	0.040	4.6	0.024
20	42.2	2		11.4	.030	4.8	.025
21	43.7	4		11.4	.038	4.6	.023
22	65.0	1		8.4	.018	3.3	.018
23	62.5	2		10.5	.025	2.0	.020
24	62.5	4		11.3	.020	3.7	.020
25	12.1	1	3.0	8.9	0.052	8.6	0.028
26	8.2	2		12.7	.135	8.5	.045
27	9.3	4		10.6	.135	6.9	.040
28	10.1	1		4.3	.050	6.0	.015
29	10.9	2		14.1	.118	6.7	.038
30	10.5	4		15.5	.115	7.7	.025
31	27.8	1	3.0	5.7	0.036	10.0	0.025
32	26.6	2		16.3	.054	7.1	.035
33	25.8	4		14.6	.055	9.1	.035
34	29.2	1		9.4	.035	8.3	.033
35	27.0	2		18.6	.055	8.7	.031
36	26.4	4		20.6	.054	9.3	.040
37	46.1	1	3.0	10.3	0.021	8.4	0.022
38	47.3	2		18.9	.027	8.6	.023
39	47.3	4		18.8	.040	10.9	.025
40	47.3	1		9.8	.025	8.5	.021
41	47.3	2		19.4	.029	7.7	.026
42	46.2	4		19.3	.035	10.2	.027
43	59.4	1	3.0	8.0	0.025	7.2	0.015
44	58.4	2		17.2	.028	10.2	.020
45	62.6	4		20.3	.025	4.8	.025
46	62.6	1		7.1	.025	10.0	.025
47	62.6	2		24.3	.024	7.1	.020
48	60.4	4		18.8	.030	6.1	.025
49	38.0	1	3.0	10.9	0.037	8.0	0.037
50	36.5	2		14.9	.054	9.4	.037
51	39.1	4		21.6	.055	8.0	.030
52	45.2	1		5.5	.020	13.2	.035
53	44.4	2		15.1	.050	9.1	.037
54	42.2	4		15.9	.060	8.3	.040
55	71.9	1	3.0	12.4	0.030	4.0	0.017
56	70.1	2		22.5	.030	7.8	.025
57	66.5	4		17.4	.032	9.7	.032
58	68.3	1		9.5	.021	10.5	.028
59	70.1	2		18.9	.032	10.6	.027
60	70.1	4		19.0	.035	9.8	.030

TABLE I.- GROUND-REACTION FORCES - Concluded

(d) Right inboard wheel

[Nose-wheel obstacles removed for tests 49 to 60]

Test number	Ground speed, V, mph	Obstacle dimensions		Force time-history characteristics			
		w, ft	h, in.	ΔF_v	t_{F_v}	ΔF_h	t_{F_h}
1	11.9	1	1.5	6.0×10^3	0.042	7.6×10^3	0.020
2	10.0	2		7.8	.114	6.5	.027
3	10.2	4		9.1	.100	6.7	.030
4	11.6	1		7.1	.060	7.8	.025
5	10.5	2		8.9	.096	6.1	.024
6	11.1	4		10.0	.087	6.1	.022
7	25.4	1	1.5	7.0	0.022	8.8	0.017
8	26.7	2		11.1	.035	7.4	.015
9	27.2	4		10.5	.039	7.7	.035
10	33.4	1		9.6	.022	8.9	.028
11	31.6	2		12.5	.032	9.4	.025
12	30.2	4		11.3	.040	7.8	.025
13	44.3	1	1.5	8.4	0.012	9.5	0.020
14	45.5	2		14.5	.021	6.8	.016
15	47.3	4		14.8	.021	5.2	.016
16	55.6	1		11.6	.014	7.6	.016
17	53.9	2		14.4	.018	11.0	.014
18	50.8	4		12.2	.021	9.2	.020
19	52.3	1	1.5	9.0	0.025	9.4	0.020
20	42.2	2		14.3	.027	7.0	.026
21	43.7	4		14.1	.025	6.2	.020
22	65.0	1		11.6	.018	6.6	.014
23	62.5	2		13.6	.015	10.5	.015
24	62.5	4		13.1	.019	8.5	.012
25	12.1	1	3.0	9.1	0.038	11.2	0.026
26	8.2	2		8.8	.125	11.9	.030
27	9.3	4		11.4	.116	9.8	.031
28	10.1	1		8.2	.036	11.6	.031
29	10.9	2		11.5	.034	13.0	.030
30	10.5	4		13.7	.103	11.0	.028
31	27.8	1	3.0	8.6	0.025	14.3	0.020
32	26.6	2		14.6	.045	12.0	.015
33	25.8	4		12.9	.045	13.1	.020
34	29.2	1		13.5	.030	14.6	.025
35	27.0	2		9.0	.039	11.9	.020
36	26.4	4		19.0	.033	13.2	.022
37	46.1	1	3.0	12.8	0.018	17.8	0.023
38	47.3	2		22.0	.025	15.9	.019
39	47.3	4		33.5	.026	14.7	.020
40	47.3	1		14.9	.020	18.8	.025
41	47.3	2		19.2	.025	15.2	.020
42	46.2	4		19.4	.025	14.8	.020
43	59.4	1	3.0	14.3	0.016	20.5	0.016
44	58.4	2		23.5	.020	17.7	.020
45	62.6	4		22.0	.025	19.2	.025
46	62.6	1		13.2	.021	19.7	.021
47	62.6	2		24.8	.020	20.9	.020
48	60.4	4		19.5	.025	18.5	.025
49	38.0	1	3.0	13.3	0.027	13.3	0.022
50	36.5	2		13.8	.057	12.5	.027
51	39.1	4		22.1	.047	12.9	.022
52	45.2	1		6.7	.015	12.0	.015
53	44.4	2		15.9	.028	14.0	.012
54	42.2	4		14.5	.040	14.3	.020
55	71.9	1	3.0	13.1	0.010	15.8	0.020
56	70.1	2		21.6	.021	16.7	.016
57	66.5	4		17.9	.024	16.9	.024
58	68.3	1		13.6	.014	16.8	.021
59	70.1	2		22.8	.027	15.2	.022
60	70.1	4		17.9	.025	16.0	.020

TABLE II.- GROUND-REACTION FORCES AND RESPONSE CHARACTERISTICS

[Nose-wheel obstacles removed for tests 49 to 60]

Test number	Ground speed, V, mph	Obstacle dimensions		Force time-history characteristics			$\frac{\Delta a}{g}$	$t_{\Delta a}$	$\frac{W\Delta a}{g\Delta F_V}$
		w, ft	h, in.	$\Delta F_{V,t}$	t_{F_V}	$\frac{\Delta F_V}{t_{F_V}}$			
1	11.9	1	1.5	22.0×10^3	0.088	250×10^3	0.20	0.054	0.761
2	10.0	2	↓	30.0	.125	240	.19	.065	.530
3	10.2	4		29.0	.130	223	.22	.057	.635
4	11.6	1		----------	-----	----------	.20	.070	-----
5	10.5	2		35.0	.115	304	.31	.042	.740
6	11.1	4		29.5	.115	256	.22	.060	.624
7	25.4	1	1.5	19.0	0.020	950	0.38	0.037	1.67
8	26.7	2		39.0	.045	866	.50	.055	1.072
9	27.2	4		36.0	.050	720	.42	.042	.975
10	33.4	1		30.0	.020	1,500	.40	.037	1.113
11	31.6	2		40.0	.040	1,000	.61	.042	1.275
12	30.2	4	↓	31.0	.045	689	.55	.052	1.483
13	44.3	1	1.5	----------	-----	----------	0.39	0.033	-----
14	45.5	2		38.5	0.020	1,925	.62	.032	1.346
15	47.3	4		36.0	.024	1,500	.62	.033	1.440
16	55.6	1		28.0	.010	2,800	.60	.032	1.790
17	53.9	2		40.0	.020	2,000	.62	.028	1.295
18	50.8	4	↓	35.0	.037	960	.66	.035	1.600
19	52.3	1	1.5	26.0	0.017	1,530	0.38	0.035	1.220
20	42.2	2		40.0	.030	1,332	.64	.030	1.340
21	43.7	4		30.5	.030	1,017	.65	.049	1.780
22	65.0	1		29.5	.010	2,950	.36	.023	1.020
23	62.5	2		33.0	.020	1,650	.56	.024	1.420
24	62.5	4	↓	29.5	.020	1,700	.45	-----	1.020
25	12.1	1	3.0	27.0	0.055	491	0.38	0.052	1.18
26	8.2	2		29.5	.145	203	.22	-----	.62
27	9.3	4		35.5	.140	254	.42	.055	.99
28	10.1	1		25.5	.060	425	.28	.050	.92
29	10.9	2		53.0	.130	407	.51	.045	.80
30	10.5	4	↓	51.0	.130	392	.48	-----	.74
31	27.8	1	3.0	28.0	0.025	1,120	0.44	0.040	1.31
32	26.6	2		47.5	.050	950	.82	.065	1.44
33	25.8	4		49.0	.055	890	.84	.060	1.43
34	29.2	1		----------	-----	----------	.62	.042	-----
35	27.0	2		58.5	.060	975	.91	.055	1.30
36	26.4	4	↓	64.0	.065	985	.89	.060	1.16
37	46.1	1	3.0	34.0	0.020	1,700	0.65	0.038	1.60
38	47.3	2		47.5	.025	1,900	1.07	.034	1.90
39	47.3	4		57.0	.030	1,900	1.26	.040	1.85
40	47.3	1		37.5	.025	1,500	.74	.041	1.65
41	47.3	2		----------	-----	----------	1.15	.031	-----
42	46.2	4	↓	63.5	.035	1,810	1.32	.045	1.74
43	59.4	1	3.0	42.5	0.025	1,700	0.70	0.035	1.37
44	58.4	2		67.5	.025	2,700	.71	.038	.88
45	62.6	4		62.5	.025	2,500	1.10	.042	1.47
46	62.6	1		42.0	.025	1,680	.86	.027	1.71
47	62.6	2		68.5	.025	2,740	1.10	.038	1.34
48	60.4	4	↓	61.5	.030	2,050	1.34	.034	1.82
49	38.0	1	3.0	37.5	0.030	1,250	0.62	0.054	1.38
50	36.5	2		49.0	.060	817	.90	.066	1.53
51	39.1	4		65.5	.060	1,090	1.05	.070	1.34
52	45.2	1		30.0	.030	1,000	.60	.038	1.67
53	44.4	2		----------	-----	----------	1.17	.050	-----
54	42.2	4	↓	56.5	.050	1,130	1.10	.055	1.62
55	71.9	1	3.0	----------	-----	----------	----	-----	-----
56	70.1	2		62.0	0.030	2,065	----	-----	-----
57	66.5	4		54.0	.035	1,540	1.27	.047	1.96
58	68.3	1		40.0	.030	1,330	.72	.038	1.50
59	70.1	2		77.5	.030	2,580	1.18	.042	1.27
60	70.1	4	↓	63.5	.030	2,120	1.25	.045	1.64

TABLE III.- SHOCK-STRUT DISPLACEMENT

[Nose-wheel obstacles removed for tests 49 to 60]

Test number	Ground speed, V, mph	Obstacle dimensions		Shock-strut time-history characteristics					
				Left gear			Right gear		
		w, ft	h, in.	$\Delta\delta_{max}$	$t\delta_{max}$	$\Delta t\delta_{max}$	$\Delta\delta_{max}$	$t\delta_{max}$	$\Delta t\delta_{max}$
1	11.9	1	1.5	0	----	----	0	----	----
2	10.0	2		.5	0.11	0.10	.1	0.19	0.06
3	10.2	4		.2	.17	.15	.6	.15	.06
4	11.6	1		.5	.12	.05	0	----	----
5	10.5	2		.7	.12	.09	.5	.16	.08
6	11.1	4		.2	.20	.09	0	----	----
7	25.4	1	1.5	0.1	0.06	0.04	0	----	----
8	26.7	2		.4	.07	.06	.3	0.07	0.05
9	27.2	4		.2	.09	.04	.4	.09	.07
10	33.4	1		0	----	----	.2	.06	.03
11	31.6	2		.3	.09	.03	.2	.04	.03
12	30.2	4		---	----	----	.4	.08	.07
13	44.3	1	1.5	0.2	0.06	0.04	0.3	0.06	0.03
14	45.5	2		.4	.06	.04	.5	.05	.03
15	47.3	4		.6	.06	.04	.5	.06	.04
16	55.6	1		---	----	----	.2	.05	.03
17	53.9	2		.4	.06	.03	.4	.06	.03
18	50.8	4		.7	.06	.05	.7	.06	.05
19	52.3	1	1.5	---	----	----	0	----	----
20	42.2	2		0.3	0.06	0.03	.4	0.06	0.03
21	43.7	4		---	----	----	---	----	----
22	65.0	1		0	----	----	.2	.08	.03
23	62.5	2		.4	.07	.03	.2	.07	.03
24	62.5	4		.8	.06	.06	.8	.06	.05
25	12.1	1	3.0	0.4	0.12	0.06	0.6	0.10	0.06
26	8.2	2		1.1	.17	.13	.6	.19	.12
27	9.3	4		.9	.15	.12	1.0	.16	.15
28	10.1	1		.8	.08	.05	.3	.09	.06
29	10.9	2		1.2	.14	.10	.9	.16	.12
30	10.5	4		1.0	.16	.10	.9	.19	.11
31	27.8	1	3.0	0.5	0.06	0.06	0.8	0.05	0.05
32	26.6	2		1.0	.08	.07	.9	.08	.07
33	25.8	4		1.2	.11	.07	1.1	.10	.08
34	29.2	1		.5	.08	.05	.4	.08	.03
35	27.0	2		1.1	.08	.07	.9	.08	.07
36	26.4	4		1.0	.10	.10	.8	.11	.10
37	46.1	1	3.0	0.2	0.06	0.02	0.5	0.06	0.04
38	47.3	2		.6	.06	.04	.9	.06	.04
39	47.3	4		1.1	.06	.05	1.1	.07	.05
40	47.3	1		0	----	----	.5	.06	.03
41	47.3	2		.5	.06	.04	.8	.06	.04
42	46.2	4		1.3	.08	.07	1.1	.08	.07
43	59.4	1	3.0	0.2	0.06	0.03	0.5	0.06	0.03
44	58.4	2		.7	.06	.04	.4	.06	.04
45	62.6	4		.9	.08	.05	.9	.06	.05
46	62.6	1		.1	.05	.03	.3	.04	.04
47	62.6	2		.6	.05	.03	.5	.06	.03
48	60.4	4		1.3	.07	.07	1.4	.07	.07
49	38.0	1	3.0	0.6	0.07	0.04	0.7	0.06	0.03
50	36.5	2		1.1	.09	.04	1.1	.07	.04
51	39.1	4		1.1	.11	.05	.9	.11	.06
52	45.2	1		.4	.06	.07	.8	.06	.06
53	44.4	2		1.1	.08	.05	1.0	.07	.05
54	42.2	4		1.2	.09	.07	1.2	.10	.07
55	71.9	1	3.0	0.3	0.05	0.05	0.1	0.04	0.04
56	70.1	2		.8	.05	.05	.6	.04	.04
57	66.5	4		1.3	.07	.07	1.0	.08	.08
58	68.3	1		.5	.04	.03	.6	.06	.03
59	70.1	2		1.0	.07	.04	.8	.07	.04
60	70.1	4		1.2	.08	.07	1.3	.08	.07

Figure 1.- Airplane used in the investigation. L-78020

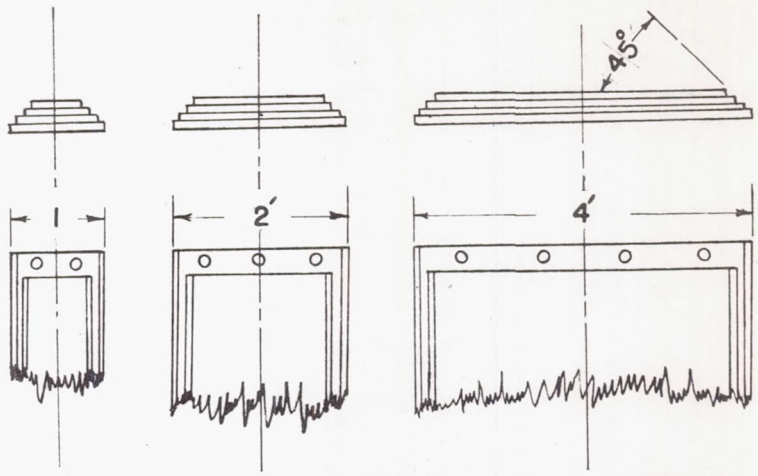

Plywood sheets 0.75 inch thick fastened together to give obstacle heights of 1.5 and 3.0 inches.

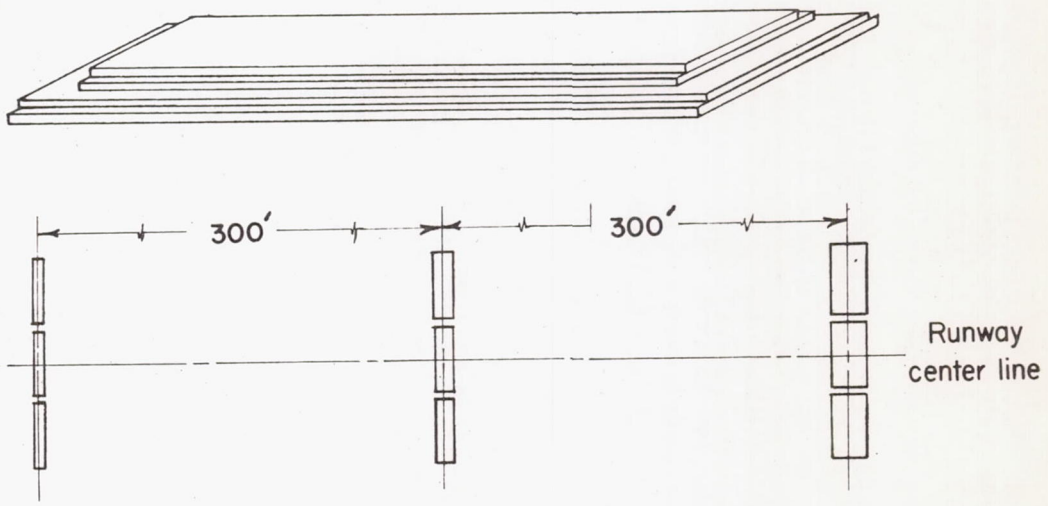

Figure 2.- Dimensions and respective positions of obstacles on the runway.

L-86775

L-86771

Figure 3.- Some test obstacles bolted to runway. h = 1.5 inches; w = 2.0 feet.

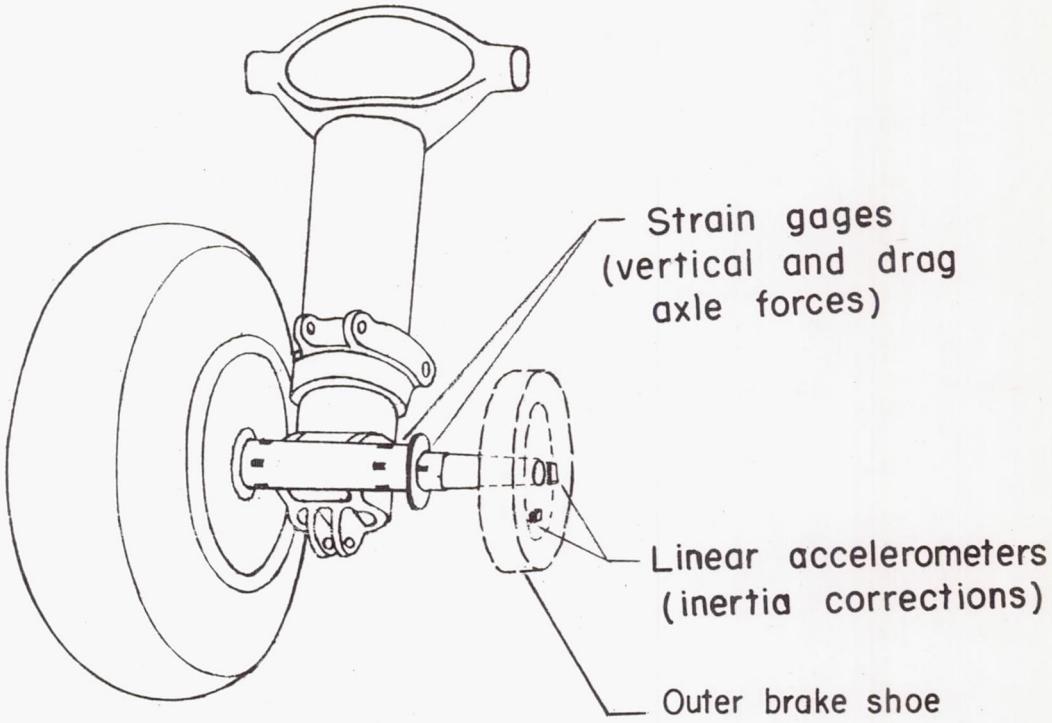

Figure 4.- Main-landing-gear truck with one wheel removed to show arrangement of instrumentation.

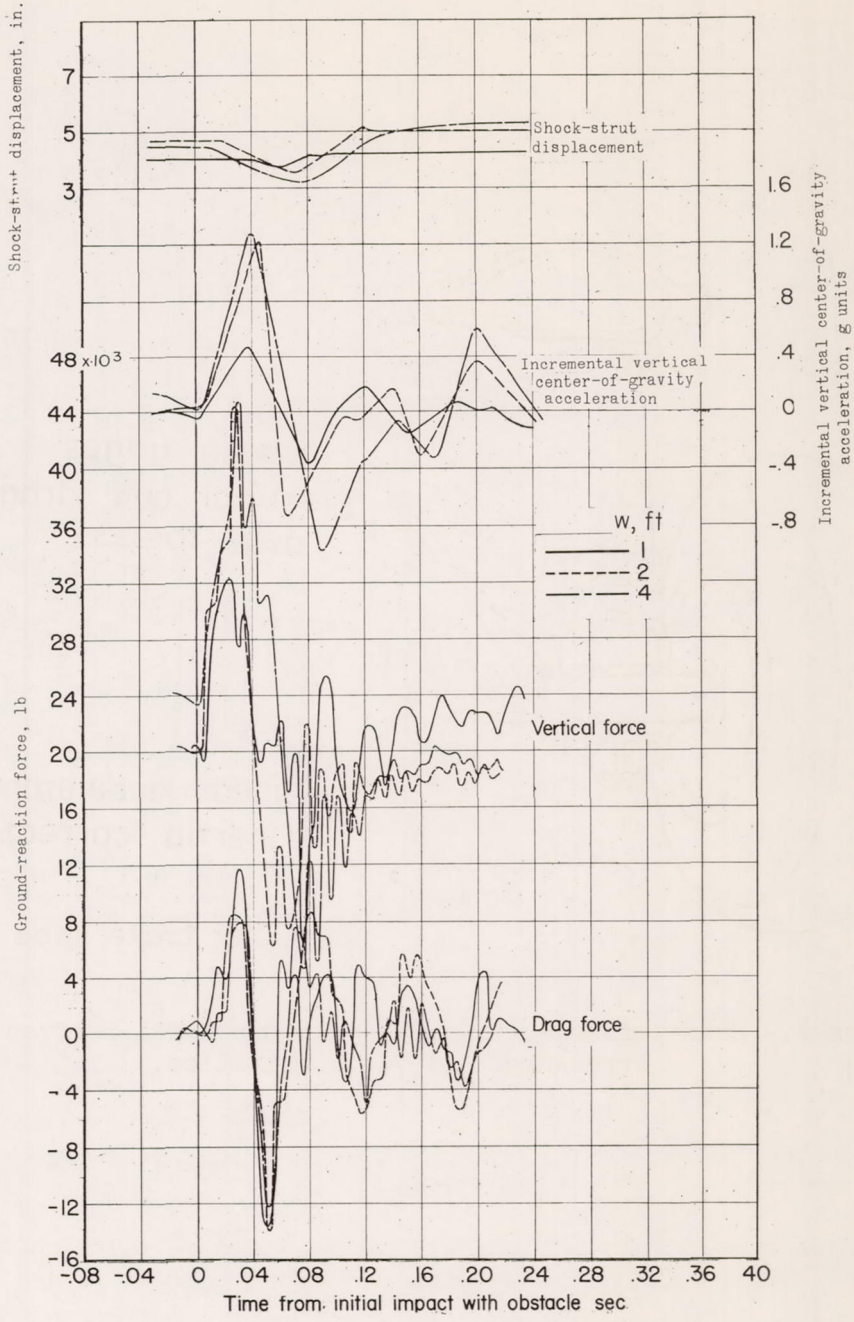

Figure 5.- Time histories of vertical and drag ground-reaction forces, center-of-gravity vertical accelerations, and shock-strut displacement for the 1-, 2-, and 4-foot-wide obstacles at approximately 70 miles per hour. h = 3.0 inches.

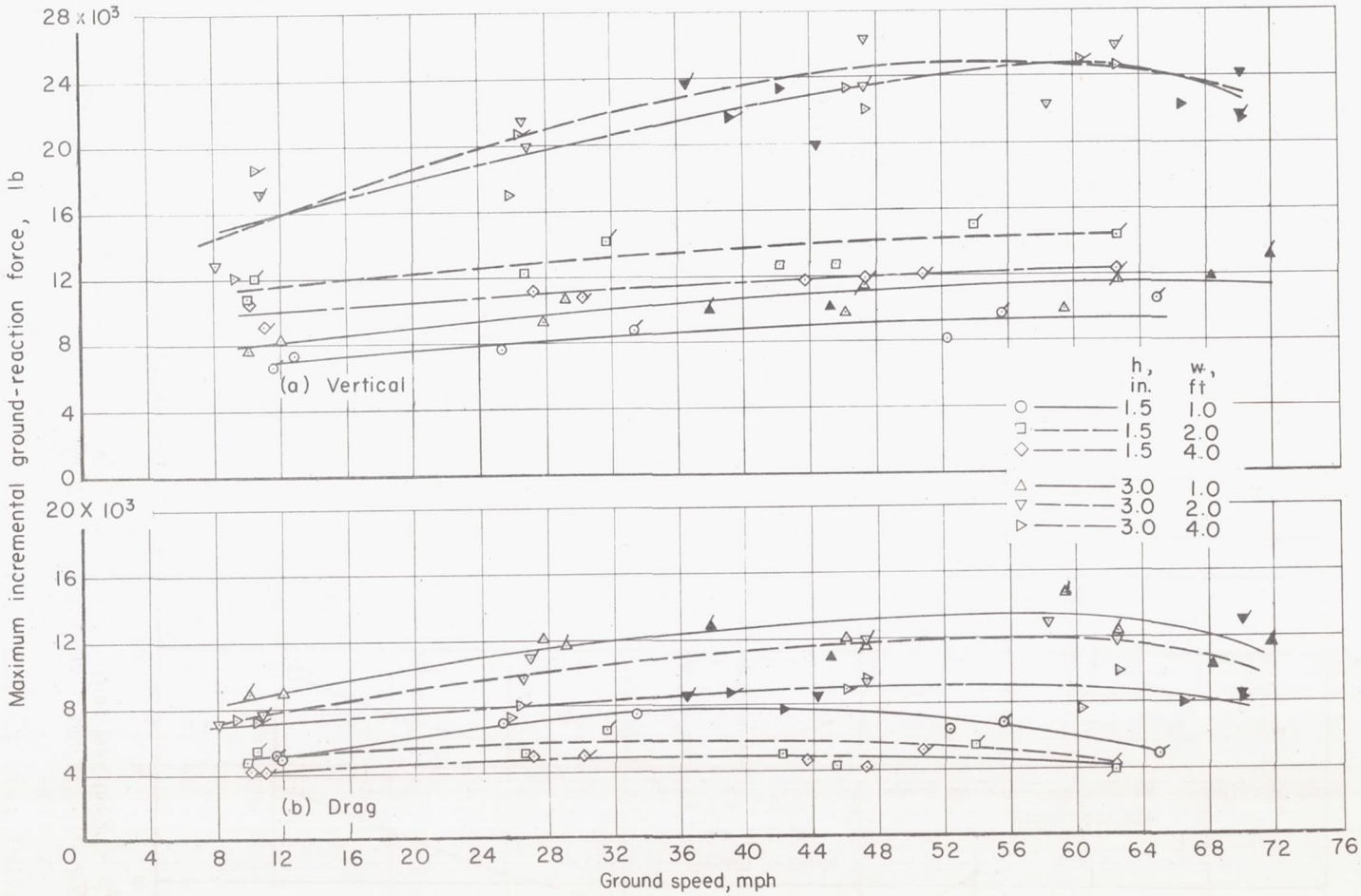

Figure 6.- Effect of ground speed on maximum incremental vertical and rearward drag ground-reaction forces for obstacles of various heights and widths. (Solid symbols designate tests with nose-wheel obstacles removed; flagged symbols designate tests made in opposite direction from those designated by unflagged symbols.)

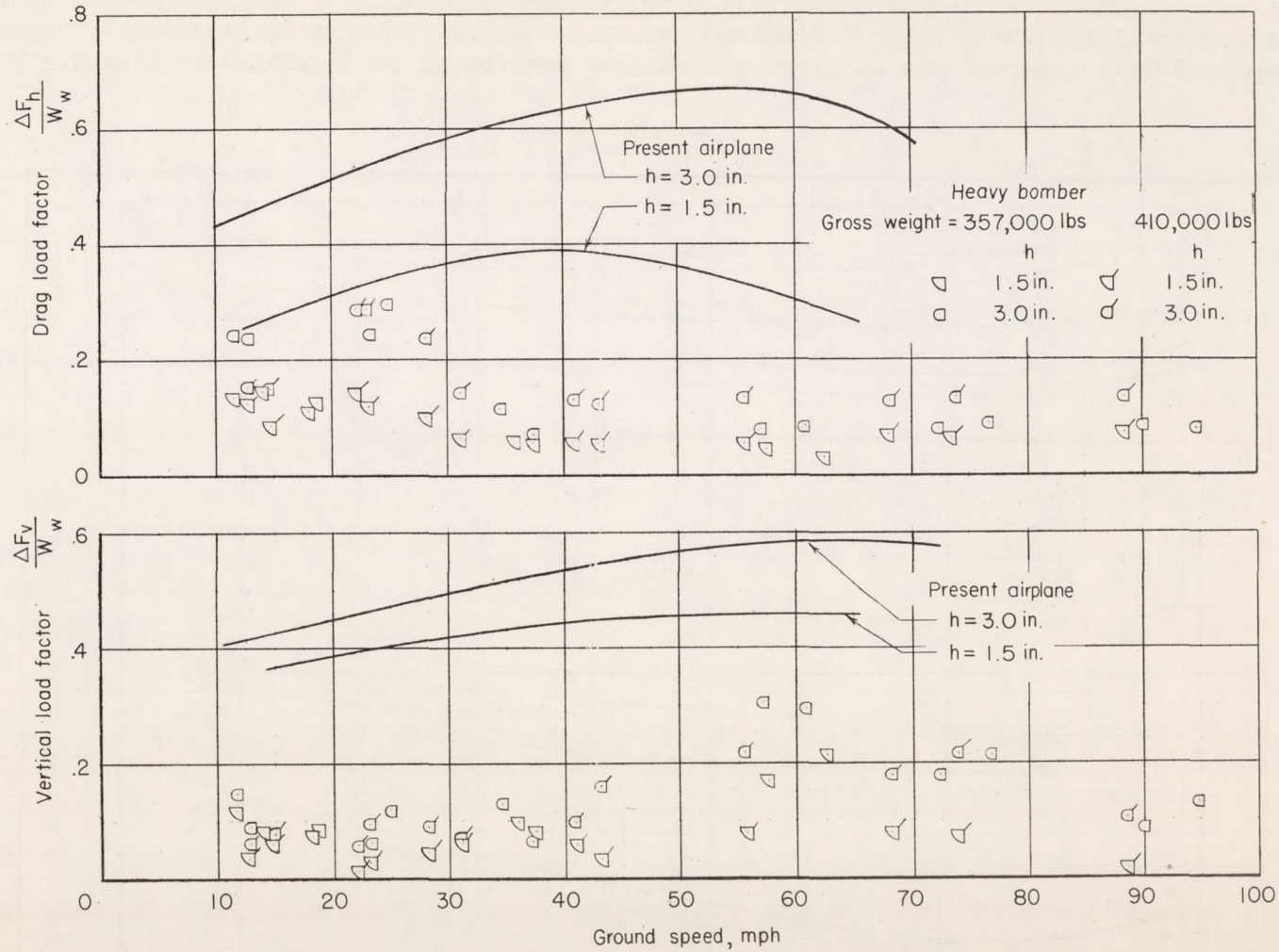

Figure 7.- Variation of vertical and drag load factors with ground speed for the tests of the present airplane compared with tests of a heavy bomber airplane when taxiing over obstacles of various heights. w = 1 foot.

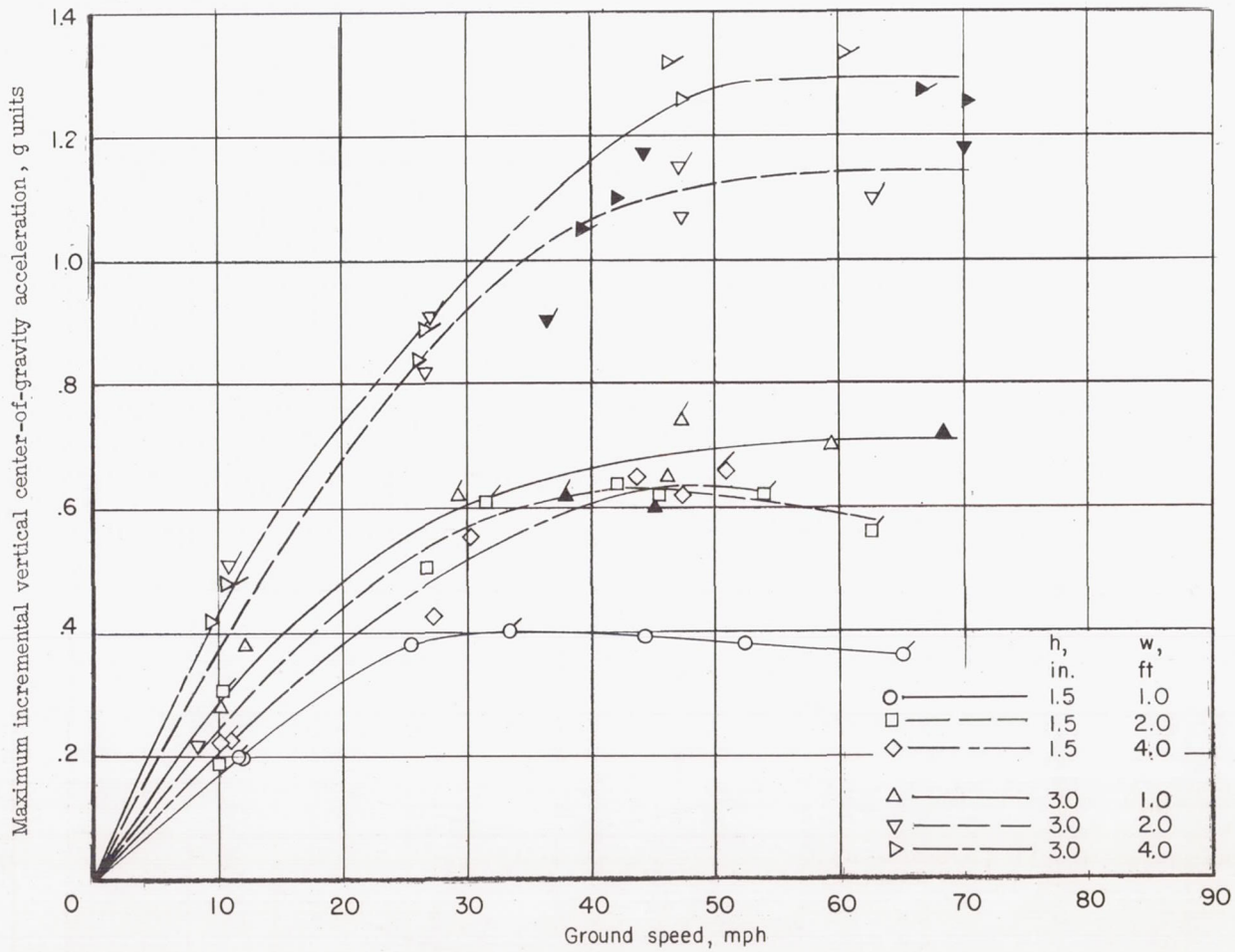

Figure 8.- Variation of maximum incremental vertical center-of-gravity acceleration with ground speed for obstacles of various widths and heights for tests of the present airplane. (Solid symbols designate tests with nose-wheel obstacles removed; flagged symbols designate tests made in opposite direction from those designated by unflagged symbols.)

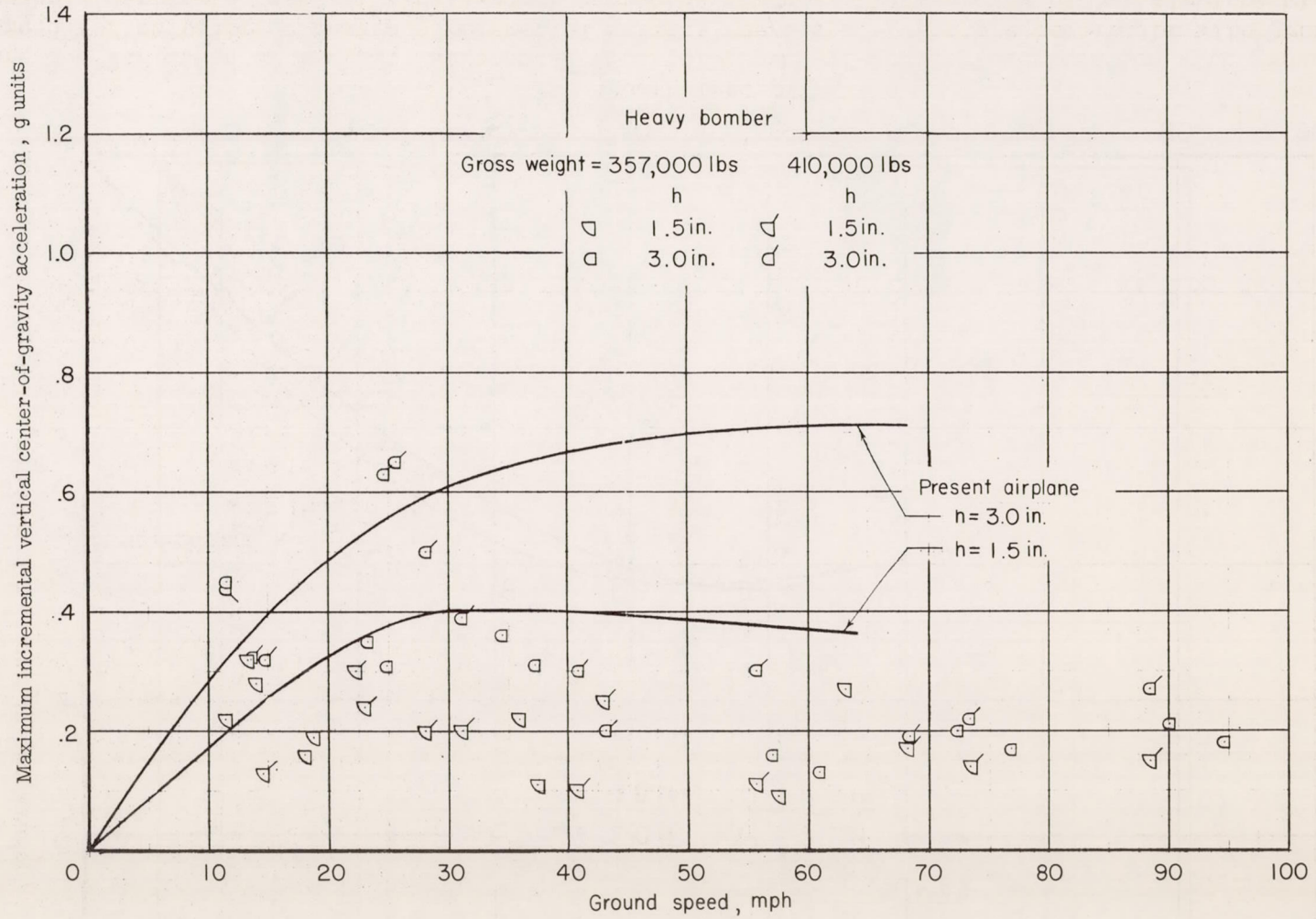

Figure 9.- Variation of maximum incremental vertical center-of-gravity acceleration with ground speed for tests of the present airplane compared with tests of a heavy bomber airplane when taxiing over obstacles of various heights. w = 1 foot.

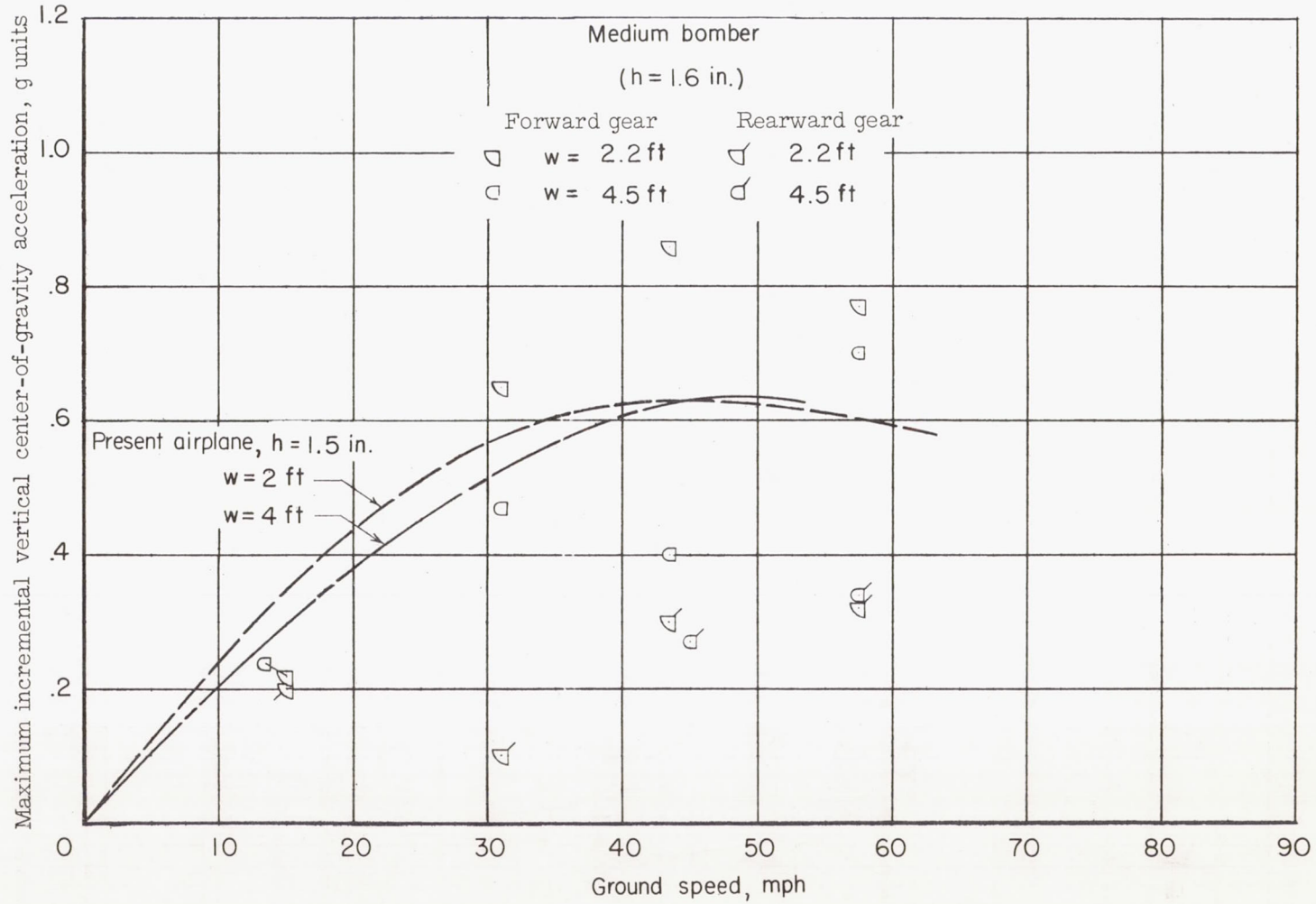

Figure 10.- Variation of maximum incremental vertical center-of-gravity acceleration with ground speed for tests of the present airplane compared with tests of a medium bomber airplane when taxiing over obstacles of various widths and heights.

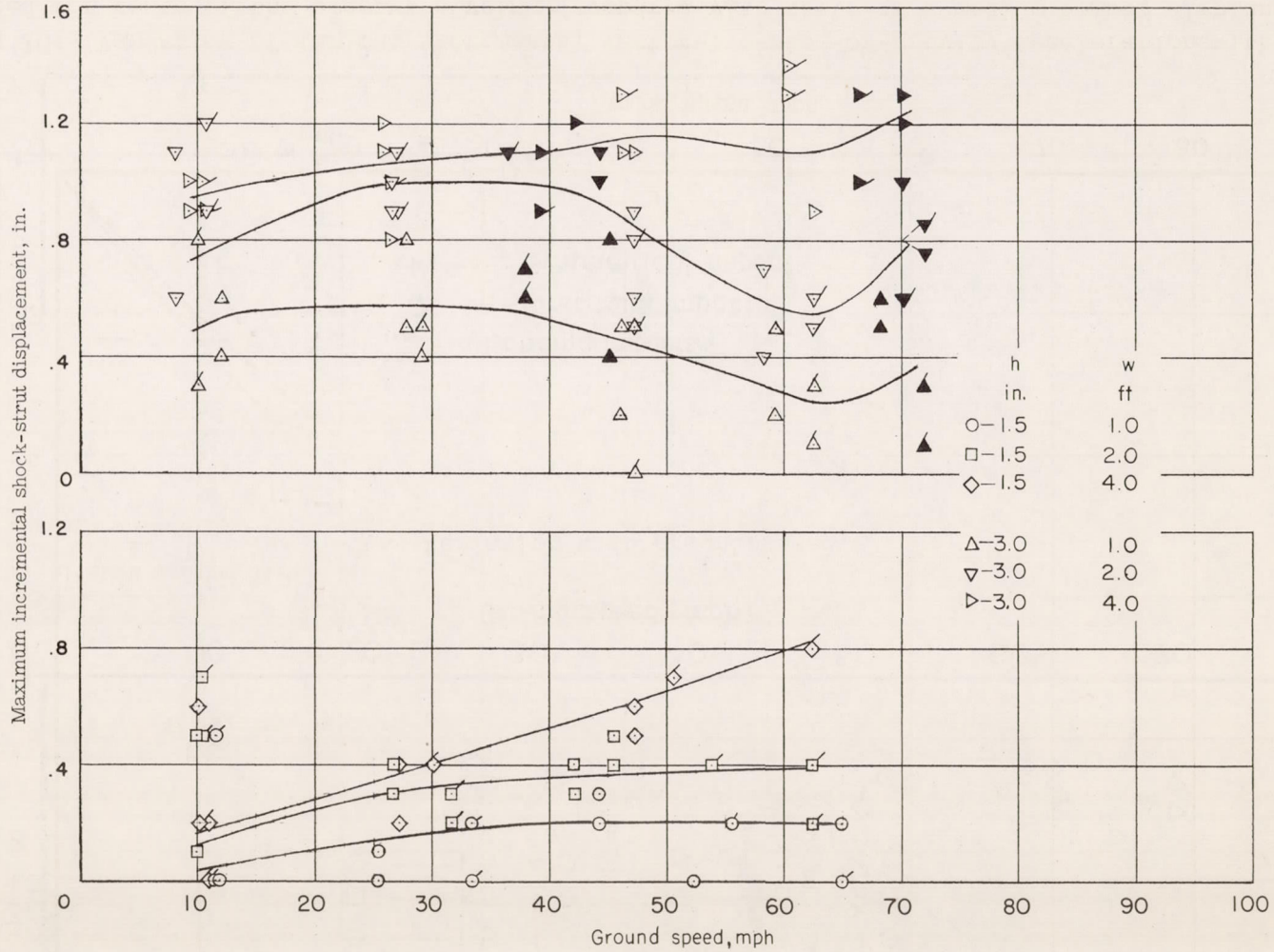

Figure 11.- Variation of maximum incremental shock-strut displacement with ground speed for tests of the present airplane when taxiing over obstacles of various heights and widths. (Solid symbols designate tests with nose-wheel obstacles removed; flagged symbols designate tests made in opposite direction from those designated by unflagged symbols.)

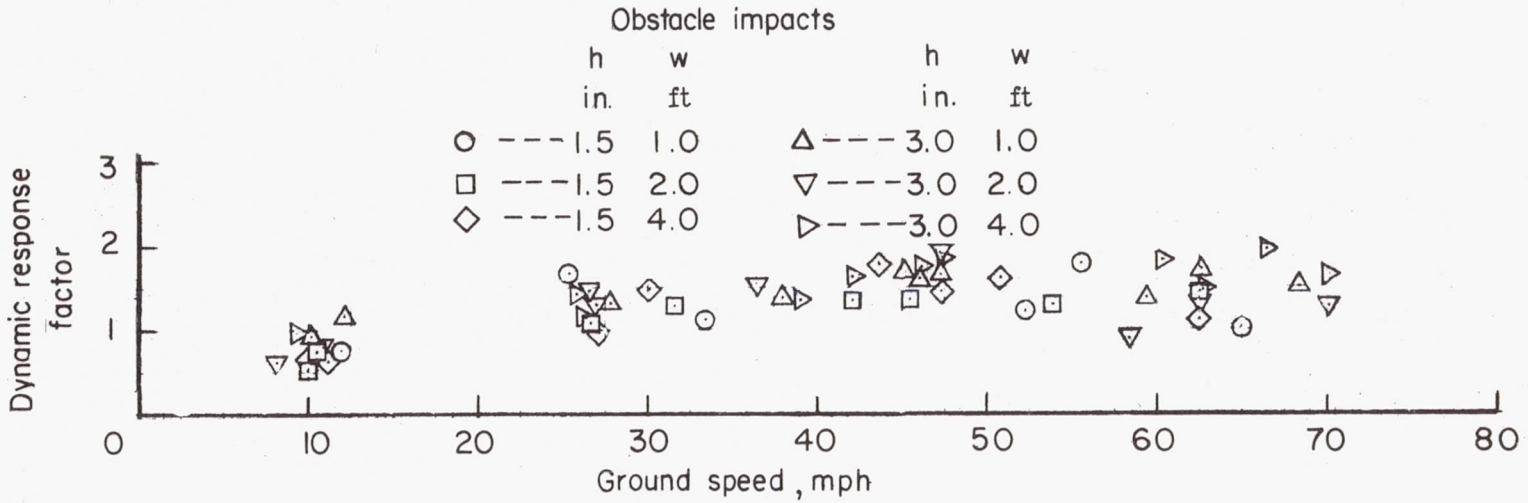

(a) Variation with ground speed.

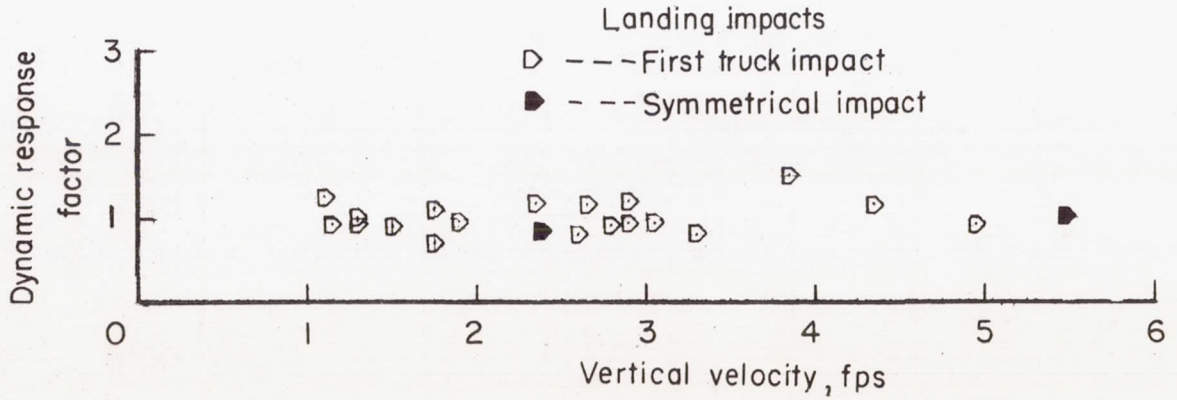

(b) Variation with vertical velocity.

Figure 12.- Dynamic-response factor.

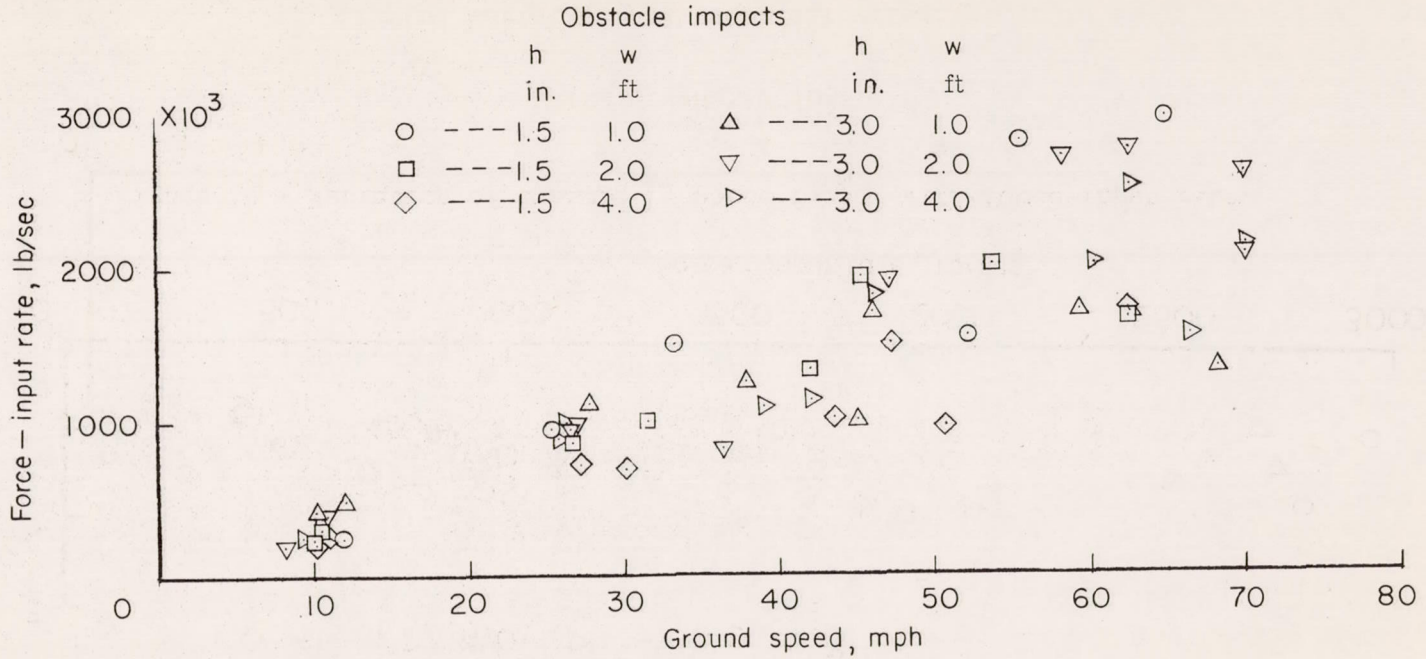

(a) Variation with ground speed.

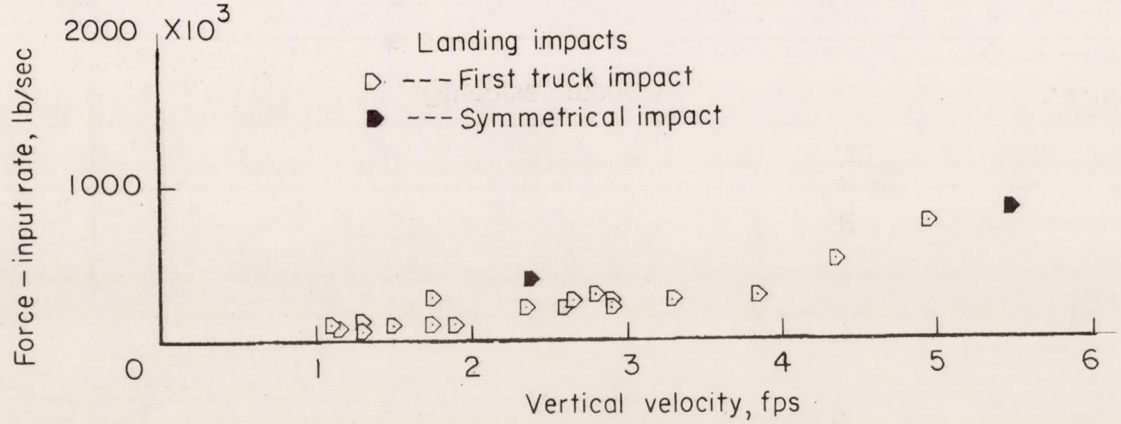

(b) Variation with vertical velocity.

Figure 13.- Force-input rate.

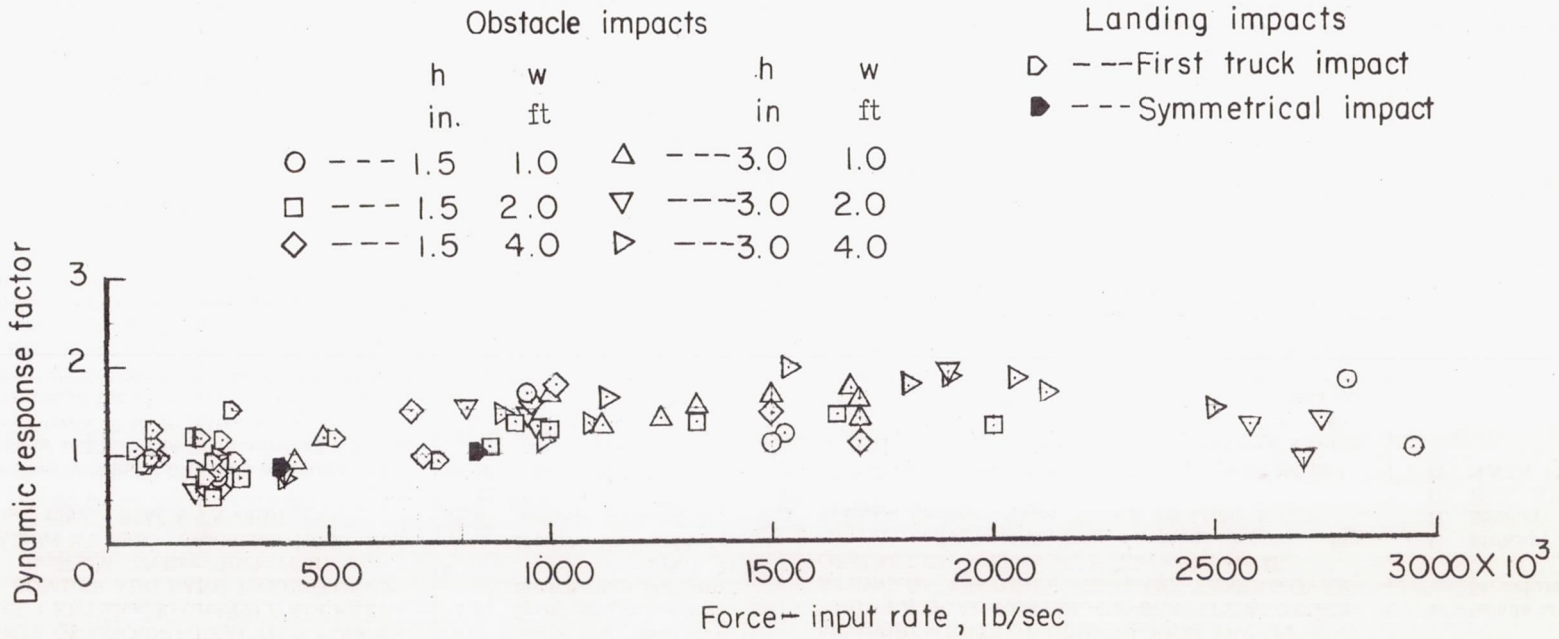

Figure 14.- Variation of dynamic response factor with force-input rate.

NACA - Langley Field, Va.